Chemical Physics Letters 457 (2008) 421–426

Contents lists available at ScienceDirect

Chemical Physics Letters

journal homepage: www.elsevier.com/locate/cplett

Observation of transition state in Raman triggered oxidation of chloroform in the ground state by real-time vibrational spectroscopy

Izumi Iwakura [a,b], Atsushi Yabushita [c], Takayoshi Kobayashi [b,c,d,e,*]

[a] JSPS Research Fellow, 8 Ichibancho, Chiyoda-ku, Tokyo 102-8472, Japan
[b] Department of Applied Physics and Chemistry and Institute for Laser Science, University of Electro-Communications, 1-5-1 Chofugaoka, Chofu, Tokyo 182-8585, Japan
[c] Department of Electrophysics, National Chiao-Tung University, Hsinchu 300, Taiwan
[d] ICORP, JST, 4-1-8 Honcho, Kawaguchi, Saitama 332-0012, Japan
[e] Institute of Laser Engineering, Osaka University, 2-6 Yamada-oka, Suita, Osaka 565-0971, Japan

ARTICLE INFO

Article history:
Received 24 October 2007
In final form 5 March 2008
Available online 10 March 2008

ABSTRACT

A transition state (TS) during Raman triggered oxidation of chloroform was directly observed by ultrafast spectroscopy using broadband visible sub-5 fs pulses. Changes in the molecular structures including the TSs along the reaction pathways were detected by the time-dependent instantaneous frequencies of vibrational modes. The Raman triggered oxidation of chloroform was found to be initiated by the excitation of vibrational levels through stimulated Raman processes involving the ground-state chloroform–oxygen complex.

1. Introduction

It was a chemists' dream for years to precisely observe the transition states (TS). However, researches in the fields of physical chemistry have recently succeeded to identify reaction intermediates and theoretical analysis helps us to investigate TS. The detailed knowledge of real chemical reactions including TSs will provide us revolutionary way to design reaction processes to improve efficiencies and varieties of products, which are hard to be found in a blind way using conventional methods. To confirm the molecular structure in the TS obtained by theoretical analysis, the direct observation of the TS during chemical reactions has been desired by chemists for many years and realized by ultrafast spectroscopy using ultrashort laser pulses. The development of NOPA (non-collinear optical parametric amplifier) [1–6] in 2002 has enabled stable generation of visible-near infrared sub-5 fs laser pulses in our group [3]. As a typical application, reaction processes including TSs were studied by detecting the structural changes using the sub-5 fs pulses [7–11]. Using the ultrashort pulses, we tried to solve the reaction mechanism by observation of the TS in a chemical reaction and supporting DFT calculation.

Chloroform is known to be easily decomposed by oxygen with sunlight, and to produce poisonous phosgene, hydrochloric acid, and carbon dioxide [12]. It is one of problem in organic synthesis processes. Furthermore, chloroform may be formed in drinking water in daily life. The knowledge chloroform reaction is important not only for the organic synthesis, but also for life hazard.

The present Letter is an extension to the Raman triggered oxidation of chloroform in the ground electric state was fully traced along the reaction pathways including TS. The analysis has been achieved by triggering the reaction through the stimulated Raman excitation of coherent distribution of vibrational levels using a broadband laser pulse of NOPA, whose spectrum is as broad as $\sim$5200 cm^{-1}. Though the reaction is ignited by an optical pulse, electronic excited states are just virtually involved.

2. Experimental

Chloroform was bubbled with nitrogen gas for 5 h to remove oxygen solved in chloroform to prepare deoxidized chloroform used as one of the samples in this work. Another sample, O_2 saturated chloroform, was prepared by bubbling with oxygen gas for 5 h to solve oxygen in chloroform. Subtracting the absorption spectrum of deoxidized $CHCl_3$ from the absorption spectrum of oxygen-dissolved samples, we found absorption peak in the vicinity of 280 nm. Therefore, it is thought that the charge-transfer complex $O_2\cdots CHCl_3$ are contained in O_2 bubbled chloroform. The width, wavelength, and repetition rate of the pulses of NOPA are sub-5 fs, 525–725 nm and 5 kHz respectively. The pump and probe intensities of the pulses are 2200 and 480 GW/cm^2, respectively. See Supplementary material for further details.

* Corresponding author. Address: Department of Applied Physics and Chemistry and Institute for Laser Science, University of Electro-Communications, 1-5-1 Chofugaoka, Chofu, Tokyo 182-8585, Japan. Fax: +81 42 443 5825.
E-mail address: kobayashi@ils.uec.ac.jp (T. Kobayashi).

0009-2614/$ - see front matter © 2008 Published by Elsevier B.V.
doi:10.1016/j.cplett.2008.03.003

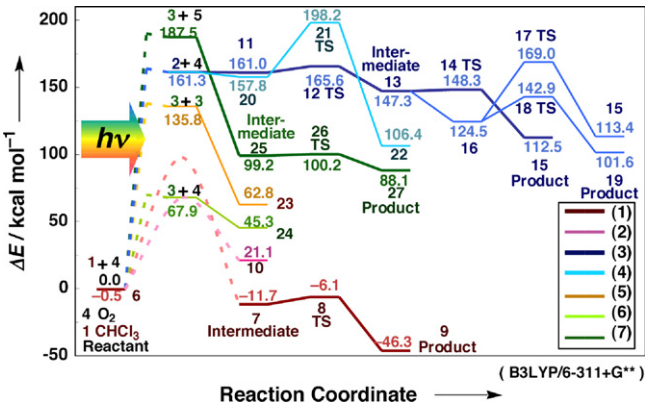

Fig. 1. Reaction pathway of photo-oxidization of chloroform estimated by B3LYP/6-31G*. Under the irradiation of light, the photon energy is converted to chemical reaction energy resulting in radical dissociation. Molecular structures of TSs for these reactions could not be estimated because of the complexity in the calculations [26]. Therefore, the images of activation energy barriers of these TSs are shown as broken curves.

3. Results and discussion

3.1. DFT calculation

3.1.1. Possible seven mechanism of photoreaction of $CHCl_3$–O_2 complex

Under light irradiation, chloroform **1** is photo-dissociated into CCl_2 **2** [13,14] and $\cdot CHCl_2$ **3** [15,16] and easily reacts with O_2 **4** and O **5** [17] to generate ClCO, CHClO, CCl_2O, etc. [18]. The C–H insertion reaction is also known as photo-oxidation of chloroform [19,20].

When chloroform and oxygen are photo-excited, the following seven reactions are possible: photo-oxidation of chloroform through C–H insertion (1) or C–Cl insertion (2) [21], reaction of CCl_2 with O_2 (3) or $CHCl_3$ (4), dimerization of $\cdot CHCl_2$ (5), and reaction of $\cdot CHCl_2$ with O_2 (6) or O (7). The results of all ground-state reactions calculated with the B3LYP/6-311+G** method [22] are shown in Figs. 1 and 2. The images of activation energy barriers of TSs, which start the reaction under light irradiation, are shown as broken curves in Fig. 1 [23].

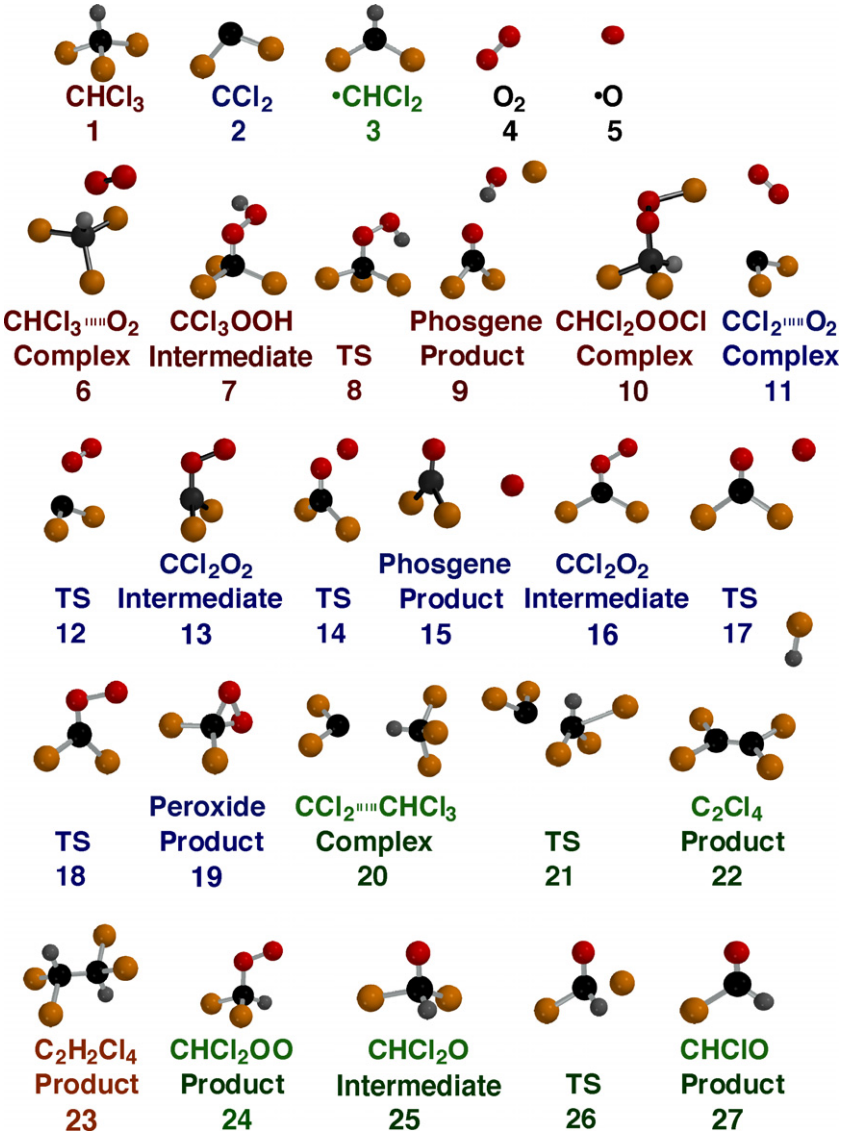

Fig. 2. Calculated structure at B3LYP/6-31G* of the species in the reaction processes discussed. In each molecular model, the Cl is colored orange, O red, C black, and H gray. (For interpretation of the references to colour in this figure legend, the reader is referred to the web version of this article.)

$$CHCl_3\ \mathbf{1} + O_2\ \mathbf{4} \rightarrow CCl_3OOH\ \mathbf{7} \rightarrow CCl_2O\cdots HO\ \mathbf{9} + Cl \quad (1)$$

$$CHCl_3\ \mathbf{1} + O_2\ \mathbf{4} \rightarrow CHCl_2OOCl\ \mathbf{10} \quad (2)$$

$$CCl_2\ \mathbf{2} + O_2\ \mathbf{4} \rightarrow CCl_2OO\ \mathbf{13} \rightarrow CCl_2O\ \mathbf{15} + O \quad (3)$$

$$CCl_2\ \mathbf{2} + CHCl_3\ \mathbf{1} \rightarrow C_2Cl_4\ \mathbf{22} + HCl \quad (4)$$

$$\cdot CHCl_2\ \mathbf{3} + CHCl_2\ \mathbf{3} \rightarrow C_2H_2Cl_4\ \mathbf{23} \quad (5)$$

$$\cdot CHCl_2\ \mathbf{3} + O_2\ \mathbf{4} \rightarrow CHCl_2OO\ \mathbf{24} \quad (6)$$

$$\cdot CHCl_2\ \mathbf{3} + O\ \mathbf{5} \rightarrow CHCl_2O\ \mathbf{25} \rightarrow CHClO\ \mathbf{27} + Cl \quad (7)$$

3.1.2. The mechanism of the photo-oxidization of chloroform (schemes (1) and (2))

As the calculated results of activation energies only scheme (1) is possible. The detail can be explained as follows.

When O_2 is dissolved in chloroform (solubility constant of O_2 in chloroform being 9.8 mM atm^{-1}) [24], O_2 is coordinated to the H of chloroform and generates a coordinated complex $CHCl_3\cdots O_2$ **6** (−0.5 kcal mol^{-1}, ~16% of the dissolved O_2 being coordinated in 6 [25]).

In case of scheme (1), under light irradiation, the photon energy is converted to chemical reaction energy and dissociates the C–H bond of $CHCl_3$. Then C–H insertion of O_2, proceeds to generate an intermediate CCl_3OOH **7** (−11.7 kcal mol^{-1}) via the TS of C–H insertion. Then, OH and Cl are dissociated from CCl_3OOH **7** with activation energy of 5.6 kcal mol^{-1} via TS **8**, and the product phosgene **9** is coordinated with dissociated OH. The imaginary frequencies of TS **8** indicate that a barrier is present along the OH rotational motion of CCl_3O–OH **7**. The intrinsic reaction coordinate were further calculated to confirm that TS **8** lies on the saddle points of the energy surface between the intermediate **7** and the product **9**. When the OH of CCl_3O–OH **7** rotates in such a way that OH approaches Cl within the distance of the van der Waals radii of OH and Cl, then these two species start to dissociate from of Cl–CCl_2O–OH **7**.

On the other hand, in case of scheme (2), C–Cl insertion of O_2, does not proceed because its intermediate $CHCl_2OOCl$ **10** is less stable than the reactant of $CHCl_3\cdots O_2$ complex **6** by 21.1 kcal mol^{-1}.

3.1.3. The mechanism of the photoreaction of CCl_2 2 (schemes (3) and (4))

The case of CCl_2 **2** generating under photo-dissociation of chloroform, as the calculated results of activation energies only scheme (3) is possible. The detail can be explained as follows.

In case of scheme (3), the generated CCl_2 **2** will react with triplet state O_2, (reactant $CCl_2 + O_2$ 161.3 kcal mol^{-1}), and a complex $CCl_2\cdots O_2$ **11** is formed (161.0 kcal mol^{-1}, triplet state). The complex **11** changes to TS **12** with 4.6 kcal mol^{-1} and an intermediate CCl_2OO **13** (147.3 kcal mol^{-1}, triplet state) in series. Then, O is dissociated from CCl_2O–O **13** via TS **14** with 1.1 kcal mol^{-1} followed by phosgene **15** being produced. It looks less stable than the reactant energy of $CHCl_3$ and O_2 by 100 kcal mol^{-1} or more because photo-dissociation products ·H and ·Cl have high energies.

In case the triplet state intermediate **13** is converted to a singlet state **16** by intersystem crossing, neither 'O-dissociated from CCl_2O–O **14** TS **17**' nor 'TS **18** react to generate dichlorocarbon peroxide **19**', because of their high activation energies of 44.5 and 18.4 kcal mol^{-1}, respectively.

If case of scheme (4), CCl_2 **2** reacts with $CHCl_3$, their complex CCl_2–$CHCl_3$ **20** (157.8 kcal mol^{-1}) is produced. However, the activation energy of TS **21** to generate CCl_2–CCl_2 **22** is so high, 40.4 kcal mol^{-1}, that the reaction is unlikely to take place.

3.1.4. The mechanism of the photoreaction of ·$CHCl_2$ 3 (schemes (5)–(7))

The case of ·$CHCl_2$ **3** generating under photo-dissociation of chloroform, as the calculated results, all schemes (5)–(7) cannot exclude. The detail can be explained as follows.

In case of schemes (5)–(7), when ·$CHCl_2$ is generated under light irradiation on $CHCl_3$, dimerization process ·$CHCl_2$ **3** producing $CHCl_2$–$CHCl_2$ **23**, scheme (5), the reaction between ·$CHCl_2$ and O_2 producing $CHCl_2OO$ **24**, scheme (6), and the reaction between ·$CHCl_2$ and O generating ·$CHCl_2O$ **25**, scheme (7), have heats of reaction of 73.0, 22.6, 88.4 kcal mol^{-1}, respectively. Radicals ·$CHCl_2$ and O react rapidly with each other to form ·$CHCl_2O$ **25.** After that, one of the ·Cl is easily dissociated with activation energy lower than 1 kcal mol^{-1} via TS **26** and changes to CHClO **27**.

3.2. Pump–probe experiment

3.2.1. Real-time trace and FFT analysis

The above theoretical calculations show that schemes (1), (3), (5)–(7) are likely to take place. We have thus used sub-5 fs pulses [2,3] to observe the real-time dynamics of the photo-oxidization of chloroform discussed above.

The oscillatory absorbance change (ΔA) signal of deoxidized chloroform around finite positive value of ΔA (Fig. 3a) is ascribed to the electronic excited state excited by multi-photon absorption. The Fourier transform (FT) of the real-time trace has peaks at 260 (δ_{C-Cl}: deformation), 366 (δ_{C-Cl}), 667 (ν_{C-Cl}: stretching), and 1237 cm^{-1} (δ_{C-H}) (Fig. 3c and d), which agree well with the corresponding Raman frequencies [26]. The signal of O_2-dissolved chloroform around 0 (Fig. 3c) indicates that there is no electronic excitation. And so, the signal observed can be concluded to be due to $CHCl_3\cdots O_2$ complex. The reason why $CHCl_3\cdots O_2$ complex was observed can be given as follows. The formation of oxygen–chloroform complex reduces the electronic transition energy from 7.3 eV (170 nm) to 4.4 eV (280 nm) by the charge-transfer interaction between chloroform and O_2. The transition of 4.4 eV is due to the charge-transfer band, which is expected to increase polarizability change upon excitation resulting in the increase in the Raman cross section. The transition is still non-resonant even after the complex formation, but the detuning energy is reduced from 4.8 to 1.9 eV than that of deoxidized chloroform, therefore $CHCl_3\cdots O_2$ complex was more efficiently observed.

Chloroform does not absorb the laser, but the sub-5 fs pulses excited vibrational levels in the ground state by stimulated Raman process, and the oxidation of O_2 coordinated complex **6** is triggered. Concerning the amount of population of the vibrational levels in the 5200 cm^{-1} range, photo-irradiation by the laser pulse is almost equivalent to thermal-irradiation at 7500 K of vibrational (non-equilibrium) temperature by the stimulated Raman process, because the laser spectrum has a broad spectral width of 5200 cm^{-1}, extending from 525 to 725 nm. Usually, the vibrational ladders can be climbed up one by one by large number of multi-photon resonant IR photons from high power laser via high-order nonlinear interaction. However, the photo-irradiation of the broadband pulse used in the present study can excite to vibrational levels equivalent to about 7500 K through the stimulated Raman process. The Raman process can excites the sample to single quanta at one time. Of course the state after the stimulated Raman excitation is not equilibrium state, in which temperature cannot be defined. However, the state has populations in the vibrational level, which can only be reached in molecular systems in equilibrium state at 7500 K.

It is impossible to excite the electronic state in chloroform by one photon absorption process even though the laser spectrum used in the present work has a broad frequency width of 5200 cm^{-1} corresponding to 7500 K. FFT amplitude of the absorbance change of O_2-dissolved chloroform is linearly proportional to the pump intensity (Fig. 4), which shows that the state to be observed is not electronic excited states excited by multi-photon absorption, but the lowest excited vibrational level of $v = 1$.

It may sound difficult to believe single quanta would trigger a chemical reaction. However, there might not be report example

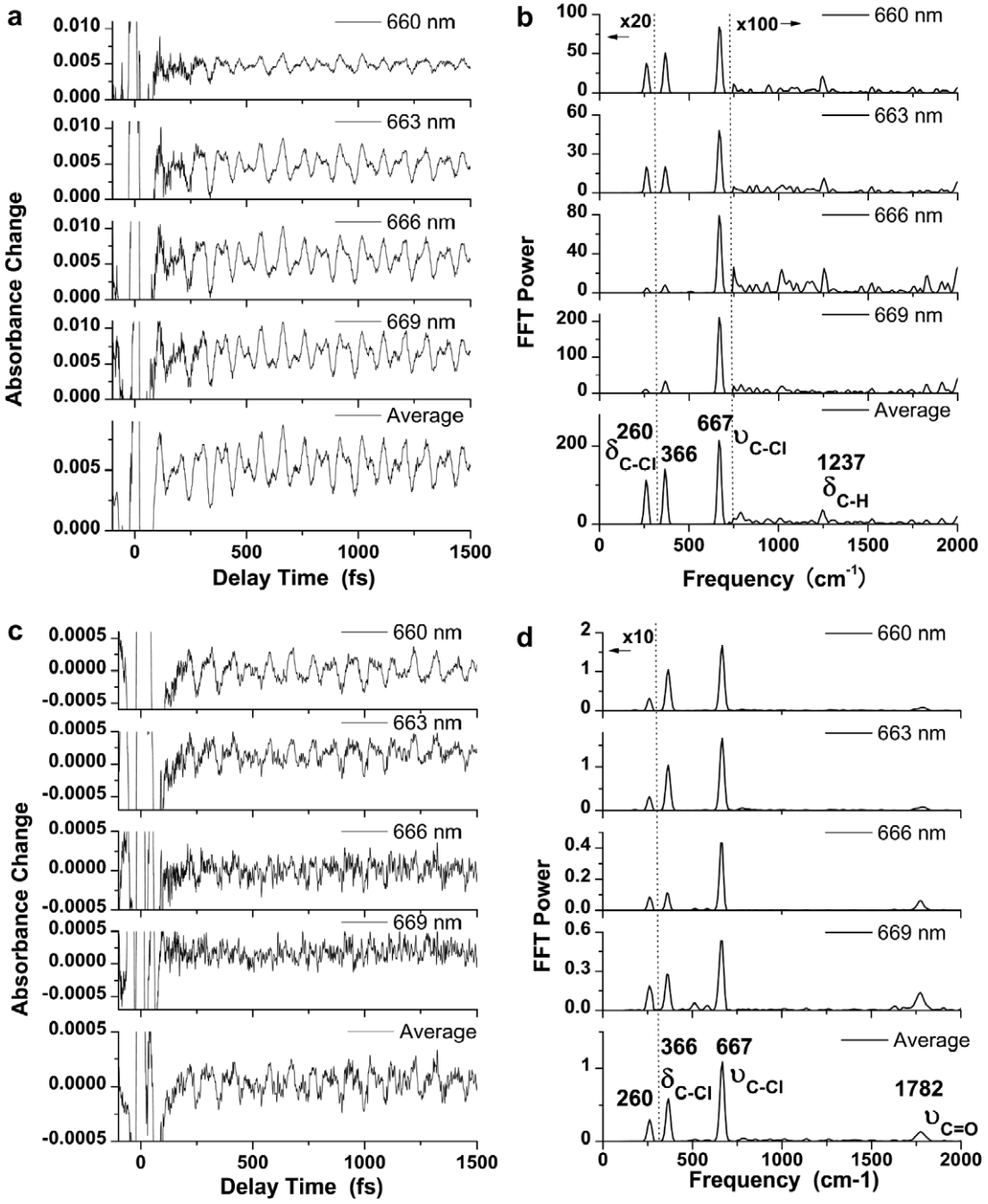

Fig. 3. Experimental results of the real-time trace of induced absorbance change probed at 660–670 nm (1.88–1.85 eV): (a) deoxidized $CHCl_3$ and (c) O_2-dissolved $CHCl_3$, and Fourier power spectra of the real-time traces in the delay time ranging 200–1500 fs: (b) deoxidized $CHCl_3$ and (d) O_2-dissolved $CHCl_3$.

of reaction triggered by single quanta, the reaction never has the positive proof of not being triggered by single quanta. The experimental result obtained in this work can be explained only by the reaction triggered by single quanta from the linearity relation between the vibrational amplitude of the $O_2\cdots CHCl_3$ and pump intensity. Because of the broad bandwidth of the laser pulse, the excitation of the vibrational modes is equivalent to the excitation by heat of 4500 K (=3000 cm^{-1}). Therefore, it is reasonable the excitation does not occur within seconds or less in the natural world at room temperature. There can be a possibility that the reaction in solution discussed in this work may take place more efficiently because of the following reasoning than that in a gas phase. Molecular vibration modulates the atomic bond length and charge on atoms. When the molecule is polarized under the modulation of the charge, surrounding solvent molecules work as a ligand and increase the bond distance, which accelerates the reaction. It shows that the solvent is converting the vibration energy into the energy for reaction. The FT signal of the O_2-dissolved chloroform has an additional peak to those of deoxidized chloroform, which is observed at 1782 cm^{-1} ($\nu_{C=O}$) (Fig. 3c and d).

3.2.2. Spectrogram analysis

The calculated spectrogram at 666 nm using the Blackman window of 240 fs FWHM shows a gradual change in the FT spectrum from the beginning of the reaction to 1300 fs after excitation. The time and frequency resolutions of the spectrogram were estimated

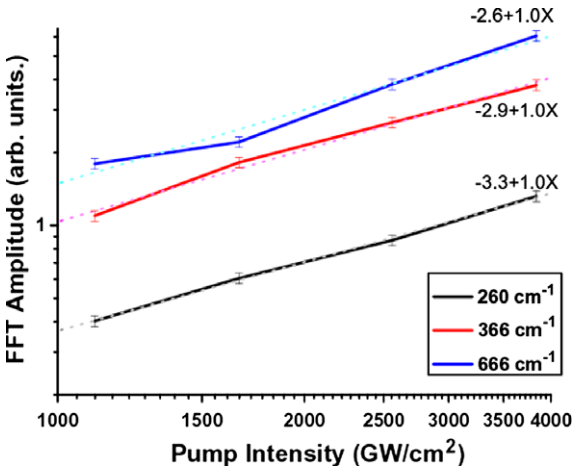

Fig. 4. Pump intensity dependence of vibrational amplitude of $CHCl_3\cdots O_2$ with the same probe intensity of 480 GW cm^{-2}.

as 100 fs and 30 cm^{-1}, respectively. The data in the vicinity of 0 fs up to ~250 fs could not be obtained with high precision because of the finite window width and the effect of interference (Fig. 5).

The spectrogram of deoxidized chloroform, Fig. 5a, shows only a small change in the red-shift of the C–H bending mode around 1237 cm^{-1} up to 1300 fs after the photo-excitation. This red-shift may be explained by the following two possible mechanisms: (1) The process of $S_{FC} \rightarrow S_R$. (2) Two modes with a small difference corresponding to a low-frequency mode of ~30 cm^{-1} around 1237 $cm^{-1}$are coupled through this low-frequency mode.

In comparison with a small change in the spectrogram of deoxidized chloroform, that of the O_2-dissolved sample exhibits a peak around 1755–1785 cm^{-1} at 600 fs after the photo-excitation (Fig. 5b). This peak can be assigned to $\nu_{C=O}$, and hence, it implies reaction between chloroform and O_2 ~ 600 fs after the photo-excitation. Fig. 3c shows that each component in this reaction process has a specific vibrational frequency.

The transfer of such vibrational coherence or even the generation of coherence by chemical reaction has also been explained previously in other systems [27–31]. The condition required for the coherence transfer is a shorter vibrational period than the vibrational dephasing time and the reaction time. The vibrational dephasing time is estimated to be longer than 100 fs from Fig. 5b. Some photo-dissociation processes can generate products without vibrations when the reaction is too fast to be measured by real-time spectroscopy. This reaction mechanism analysis observes the dynamics change of molecular structure by detecting the time-dependent instantaneous frequencies of vibrational modes. The analysis method can only detect a process slower than a molecular vibration period. Hereafter, we discuss only the processes observed on the spectrogram (Fig. 5a).

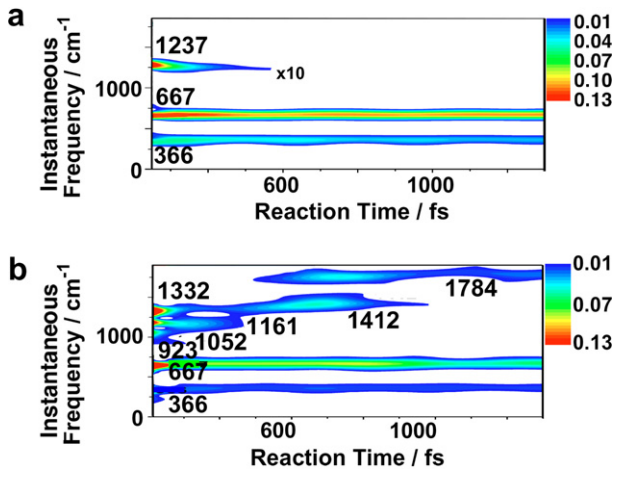

Fig. 5. Spectrograms calculated from the ΔA trace probed at 666 nm using the Blackman window function whose FWHM is 240 fs: (a) deoxidized $CHCl_3$ probed at 666 nm (1.86 eV) and (b) O_2-dissolved $CHCl_3$ probed at 666 nm (1.86 eV).

3.3. Comparison of the experimental results and calculated results

The reaction dynamics can be explained by comparison of the experimental results with the following five calculated processes. Scheme (5) and (6) can be excluded because of the lack of C=O generation. The spectrograms to be observed under schemes (1), (3), and (7) were predicted by calculations as follows (Table 1) [32].

Scheme (1): The vibration frequencies of $CHCl_3\cdots O_2$ **6** do not change significantly from those of the reactant. Light irradiation to **6** starts C–H insertion, and generates CCl_3OOH **7** gives ν_{O-O}, ν_{C-O}, and δ_{O-H} around 910, 1025, and 1400 cm^{-1}, respectively. Then, it is converted to TS **8**, which thereafter dissociates OH and Cl, and ν_{C-O} and δ_{O-H} are observed at 1090 and 1435 cm^{-1} (both blue-shifted), respectively. Then ν_{O-O} vanishes, because it is an imaginary frequency mode of the TS. Finally, product phosgene **9** gives $\nu_{C=O}$ around 1773 cm^{-1} (as for $\nu_{C=O}$, our calculated frequencies were rescaled for comparison with the experimental results [33–35] with a scaling factor of 0.96 for $\nu_{C=O}$).

The experiment spectrogram result is not contradicted by scheme (1).

Scheme (3): In the reaction of CCl_2 **2** and O_2, ν_{C-Cl} and δ_{C-Cl} of $CCl_2\cdots O_2$ **11** are blue-shifted from those of CCl_2. Then, **11** changes to TS **12** and ν_{O-O} appears around 1435 cm^{-1} because O=O in $CCl_2\cdots O{=}O$ **11** is converted to the O–O in CCl_2O–O **13** via TS **12**. In **13**, the appearance of ν_{C-O} around 1050 cm^{-1} and the symmetry of **13** cause the disappearance of ν_{O-O}. No peak appears in the range higher than 1050 cm^{-1}. Likewise, the frequency of ν_{C-O} (1182 cm^{-1}) is also the highest frequency in TS **14**. The final product phosgene **15** shows $\nu_{C=O}$ around 1809 cm^{-1} (the scaling factor for $\nu_{C=O}$ being 0.96).

The absence of signal corresponding to $\nu_{O=O}$ (1635 cm^{-1}) of $CCl_2\cdots O_2$ **11** with longer lifetime than that of CCl_2OO **13** rules out the possibility of scheme (3). Furthermore, the existence of the mode whose frequency is higher than 1182 cm^{-1} in the spectrogram also verifies that scheme (3) does not take place.

Table 1
Calculated wavenumbers of eight vibrational modes of molecules relevant in the reactions[a]

Molecule	Wavenumbers (cm^{-1})							
	$\nu_{C=O}$	$\nu_{O=O}$	δ_{O-H}	δ_{C-H}	ν_{C-O}	ν_{O-O}	ν_{C-Cl}	δ_{C-Cl}
1				1248			663	365
4		1571						
6		1573		1255			663	365
7			1343		1026	913	546	
8			1378		1090		529	
9	1773						579	307
2							660	299
11		1571					708	329
12						1436	659	320
13					1051			
14					1182			
15	1809						555	302
3				1251			748	
25				1261	1132		679	
26				1287	1327		695	
27	1773			1330			721	

[a] Wavenumbers are rescaled using a literature-based scaling factor [32].

Scheme (7): In ·$CHCl_2$ **3**, ν_{C-Cl} and δ_{C-Cl} appear around 750 and 1250 cm^{-1}, respectively. After react O, newly generated ν_{C-O} around 1130 cm^{-1} of the intermediate ·$CHCl_2O$ **25** is then blue-shifted up to 1330 cm^{-1} in ·Cl···CHClO TS **26**. Another final product CHClO **27** shows $\nu_{C=O}$ and δ_{C-H} around 1773 and 1330 cm^{-1}, respectively (scaling factor for $\nu_{C=O}$ being 0.96).

And so, the observed signal around 1410 cm^{-1} cannot be explained. In addition, generation of ·$CHCl_2$ **3** and O from the same $CHCl_3\cdots O_2$ **6** seems improbable, because each radical generation is a multi-photon process. Therefore, ps timescale diffusion in the solvent has to be considered for scheme (7), which cannot explain the reaction of 600 fs shown in Fig. 5b.

Therefore, the change observed around 600 fs after the photo-excitation in the experimental result is most likely due to the C–H insertion process, scheme (1). The calculated results of scheme (1) described earlier and the experimentally observed spectrograms can be construed as follows. At 250 fs after the photo-excitation, the intermediate CCl_3OOH **7** was generated. Because, the peaks observed at 923, 1050, 1220, and 1330 cm^{-1} were assigned to ν_{O-O} in **7**, ν_{C-O} in **7**, δ_{C-H} in $CHCl_3$, and δ_{O-H} in **7**, respectively. After that, the signal of 923 cm^{-1} (ν_{O-O}) vanished because it is an imaginary frequency mode of the TS **8** and the signals of 1050 (ν_{C-O}) and 1330 cm^{-1} (δ_{O-H}) were blue-shifted to dissociate OH and Cl in TS **8**, as predicted by the calculation. At ~600 fs after the photo-excitation, a new peak appeared at 1755 cm^{-1}($\nu_{C=O}$), and then it was gradually blue-shifted. This shift can be ascribed to the increase in $\nu_{C=O}$ as OH dissociates away from $CCl_2O\cdots OH$ **9**. The δ_{C-Cl} (307 cm^{-1}) and ν_{C-Cl} (578 cm^{-1}) of the product phosgene **9** were not observed; this is probably because the signal strengths are weak and overlapped with the strong broad signal of chloroform in these frequency regions.

4. Conclusion

Raman triggered oxidation of chloroform has been observed by ultrafast time-resolved spectroscopy using sub-5 fs pulses. Though chloroform has no absorption band in the spectral range of this laser, the broadband pulse excited the vibrational modes in the ground state by stimulated Raman processes via virtual excitation of the electronic state, and the reaction between chloroform and oxygen was triggered by the population of these vibrational levels. An analysis of the spectrogram enabled direct observation of the real-time dynamics of the oxidation process. These results have demonstrated that the observation of transition states by sub-5 fs time-resolved spectroscopy is applicable for 'ground-state reaction' as well as 'excited state reaction' via Raman excitation in a wide variety of chemical reactions.

Acknowledgments

This work was partially supported by JSPS to I.I., and a Grant MOE ATU Program in NCTU to A.Y. and T.K. The authors are grateful to the ITC of the UEC for their support of the DFT calculations.

Appendix A. Supplementary material

Supplementary data associated with this article can be found, in the online version, at doi:10.1016/j.cplett.2008.03.003.

References

[1] A. Shirakawa, I. Sakane, M. Takasaka, T. Kobayashi, Appl. Phys. Lett. 19 (1999) 2268.
[2] A. Baltuska, T. Kobayashi, Appl. Phys. B 75 (2002) 427.
[3] A. Baltuska, T. Fuji, T. Kobayashi, Opt. Lett. 27 (2002) 306.
[4] G. Cerullo, M. Nisoli, S. De Silvestri, Appl. Phys. Lett. 71 (1997) 3616.
[5] T. Wilhelm, J. Piel, E. Riedle, Opt. Lett. 22 (1997) 1494.
[6] J. Piel, M. Beutter, E. Riedle, Opt. Lett. 25 (2000) 180.
[7] T. Kobayashi, T. Saito, H. Ohtani, Nature 414 (2001) 531.
[8] T. Kobayashi, H. Wang, Z. Wang, T. Otsubo, Chem. Phys. Lett. 426 (2006) 105.
[9] T. Kobayashi, H. Wang, Z. Wang, T. Otsubo, J. Chem. Phys. 125 (2006) 044103.
[10] Z. Wang, T. Otsubo, T. Kobayashi, Chem. Phys. Lett. 430 (2006) 45.
[11] T. Kobayashi, A. Yabushita, T. Saito, H. Ohtani, M. Tsuda, Photochem. Photobiol. 83 (2007) 363.
[12] N. Schoorl, L.M. Berg, Chem. Centr. II (1905) 1623.
[13] M.L. Azcárate, E.J. Quel, J. Phys. Chem. 93 (1989) 697.
[14] V.M. Freytes, J. Codnia, M.L. Azcárate, Photochem. Photobiol. 81 (2005) 789.
[15] W.H.S. Yu, M.H.J. Wijnen, J. Chem. Phys. 52 (1970) 2736.
[16] A.J. Eskola, W.D. Geppert, M.P. Rissanen, R.S. Timonen, L. Halonen, J. Phys. Chem. A 109 (2005) 5376.
[17] B. Walker, M. Saeed, T. Breeden, B. Yang, L.F. DiMauro, Phys. Rev. A 44 (1991) 4493.
[18] H. Hou, B. Wang, Y. Gu, J. Phys. Chem. A 103 (1999) 8075.
[19] A.M. Clover, J. Am. Chem. Soc. 45 (1923) 3133.
[20] S. Gab, W.V. Turner, Angew. Chem. Int. Ed. Engl. 24 (1985) 50.
[21] M.G. Rosenberg, U.H. Brinker, J. Org. Chem. 68 (2003) 4819.
[22] Gaussian 03, Revision D.02, Gaussian, Inc., Wallingford CT, 2004.
[23] K.A. Black, S. Wilsey, K.N. Houk, J. Am. Chem. Soc. 125 (2003) 6715.
[24] B.M. Monroe, Photochem. Photobiol. 35 (1982) 863.
[25] H. Tsubomura, R.S. Mulliken, J. Am. Chem. Soc. 82 (1960) 5966.
[26] W.G. Rothschild, G.J. Rosasco, R.C. Livingston, J. Chem. Phys. 62 (1975) 1253.
[27] J.M. Jean, G.R. Fleming, J. Chem. Phys. 103 (1995) 2092.
[28] F. Rosca, A.T.N. Kumar, X. Ye, T. Sjodin, A.A. Demidov, P.M. Champion, J. Phys. Chem. A 104 (2000) 4280.
[29] M.H. Vos, F. Rappaport, J.-C. Lambry, J. Breton, J.-L. Martin, Nature 363 (1993) 320.
[30] R.J. Stsnley, S.G. Boxer, J. Phys. Chem. 99 (1995) 859.
[31] Q. Wang, R.W. Schoenlein, L.A. Peteanu, R.A. Mathies, C.V. Shank, Science 266 (1994) 422.
[32] A.P. Scotto, L. Radon, J. Phys. Chem. 100 (1996) 16502.
[33] H. Schnöckel, R.A. Eberlein, H.S. Plitt, J. Chem. Phys. 97 (1992) 4.
[34] D.L. Joo, D.J. Clouthier, A.J. Merer, J. Chem. Phys. 101 (1994) 31.
[35] E.A. Wade, K.E. Reak, B.F. Parsons, T.P. Clemes, K.A. Singmaster, Chem. Phys. Lett. 365 (2002) 473.